Comparisons between Model Forecast and Observed Boundary Layer Profiles and Related Comments on Cloud Prediction

J. D. PRICE AND M. R. BUSH

Met Office, Exeter, Devon, United Kingdom

(Manuscript received 8 March 2004, in final form 16 June 2004)

ABSTRACT

In this study comparisons are made between Met Office mesoscale model boundary layer profiles, and radiosonde data collected in the central United Kingdom during three intensive boundary layer cloud experiments. Significant differences between forecast and observed profiles were found. An assessment of whether these differences are dominated by sonde random error or model error is performed. Results suggest that sonde random errors are insignificant for stratocumulus fields, but not for cumulus ones.

Results show that model fields do not represent the fine vertical structure seen in the observations. The impact of this result for cloud prediction is discussed, and an estimate for the vertical resolution required to adequately parameterize the cloud field is provided.

1. Introduction

Numerical models face a particularly difficult task when forecasting cloud parameters. Because many cloud processes occur at scales smaller than those of typical model horizontal resolutions, it is normal to predict cloud variables via a subgrid-scale parametrization. These may be diagnostic in nature (e.g., Sommeria and Deardorff 1977; Smith 1990; Ricard and Royer 1993), where cloud variables are calculated directly from grid-box mean values of temperature, humidity, etc., at each time step, or prognostic in nature. Prognostic schemes (e.g., Tiedke 1993; Gregory et al. 2002) carry cloud variables across time steps, and an increment is calculated and added at each time step. These schemes have the advantage that they implicitly include the net effect of processes occurring at previous time steps for each time step. A comprehensive disscussion of various cloud parametrizations and their strengths and weaknesses can be found in Gregory et al. (2002). However, regardless of the parametrization type, a key element to their success is that the mean model fields that are used to initialize them must be of a sufficient quality. In fact, one can argue that the more complex a parametrization is and the wider range of conditions it is able to accurately represent, then the more accurate the initialization needs to be, because it is likely to be more sensitive to those data (this is particularly true for prognostic schemes that can suffer from stability problems). Accurate profiles of temperature and humidity are, therefore, desirable.

In this study we examine comparisons between the Met Office mesoscale model, and radiosonde data collected during three case study experiments designed to observe the evolution of boundary layer cloud. Particular attention is paid to how well the model represents the boundary layer top and/or inversion base region, because this is where most boundary layer cloud is observed (usually forming there first, and evaporating there last). A possible limiting factor to model performance in this region is its vertical resolution, which is considered in the comparison. In addition, the accuracy of the analysis fields used to initialize the forecasts is considered. The results are discussed in the context of cloud forecasting and parametrization.

Section 2 describes the observational data used in the study. Section 3 presents the comparison between observations and model forecast and analysis profiles. Section 4 discusses radiosonde random errors, and section 5 discusses resolution issues. The summary is section 6.

2. Description of data

Data used for this study were collected during various field campaigns conducted in the United Kingdom by the Met Office Research Unit at Cardington, Bedfordshire. Experiments were of the following two types: tethered balloon or radiosonde. The former (typical examples of which can be seen in Price 1999) are used to provide turbulence statistics of temperature and humidity as described in section 4. The radiosonde experiments are used to provide a detailed series of profiles.

Corresponding author address: J. D. Price, Met Office Research Unit, Cardington Airfield, Shortstown, Bedfordshire MK42 0SY, United Kingdom.
E-mail: jeremy.price@metoffice.gov.uk

On most days (when there was significant wind) these took the form of a Lagrangian analysis, whereby a mobile radiosonde unit was deployed directly up- or downwind of the main site, and released a number of sondes (typically from six to eight) at 1-h intervals. The distance of the remote location was set so that air took 2 h to travel between the sites. Sondes were released at the main site to coincide with the remote releases. In this way, tracking the development of the boundary layer at hourly intervals with a resolution of 2 h was possible. On days with light winds (less than 3 m s^{-1} in the boundary layer) only local sonde ascents were performed. In addition, the main site was instrumented with a cloud-base recorder, passive microwave radiometer, and a suite of surface instruments to measure temperature and humidity fluxes at various heights.

Three days were selected for the model comparison, chosen to show a range of convective activity. The most convective (occurring on 14 September 2001, hereafter denoted CUM) was a cumulus field that developed from clear air during a northerly outbreak on the edge of an anticyclone. The second case (occurring on 25 September, hereafter SCC), was a fog/stratus layer that developed into a moderately convective boundary layer once the solar insolation increased during the morning. At that point the cloud became stratocumulus, which subsequently dissipated. The third case (occurring on 2 November, hereafter SCQ), was a winter stratocumulus cloud deck that was weakly and intermittently coupled to the surface. It, therefore, showed only weak convective activity. Later in the day, once decoupled (i.e., once convection had died away), it took on the typical appearance of a radiatively cooling cloud layer, showing the hexagonal-type cellular structure.

3. Model comparisons

In this section we present vertical profiles of temperature and dewpoint from the Met Office mesoscale model with radiosonde data. The comparison is qualitative in nature and is designed to identify any broad difference or trends between the two datasets. We do not attempt to assess the operational model in detail, but investigate from where the major errors in representing and forecasting cloud are likely to originate.

For all 3 days presented here, it is noted that the general synopsis and performance of the model was good. That is, the larger-scale synoptic flow was well forecast. The discrepancies between the model and observations described below, therefore, originate from the small-scale representation of local conditions. A further point is that the analyses used in this study were uninitialized, which means that only half of the assimilation increments are applied to the analysis. This means that the full weighting of the observations is not used. The results presented here may, thus, differ from the operational model, though the differences are not expected to be large. Each experiment is discussed, in turn, below.

a. Description of forecast model

The Met Office Unified Model is a gridpoint model that is run operationally in a number of configurations, including climate, global forecast and U.K. mesoscale. In August 2002 a nonhydrostatic, semi-Langrangian version of the mesoscale model was introduced operationally, and a preoperational version of this model was used in this investigation. The model uses a semi-implicit time integration with an Arakawa C grid in the horizontal and a Charney–Philips grid in the vertical (Staniforth et al. 2002). It is run with a 5-min time step (although radiation is only called hourly due to its cost) and has 38 levels in the vertical, with 13 of these in the boundary layer. There are 146 $\times$ 182 points in the horizontal, giving a resolution of 12 km with a domain that covers the United Kingdom, and parts of Norway and France.

The model uses a nonlocal boundary layer scheme (Lock et al. 2000) that has an explicit entrainment parametrization and represents both top-down and surface-based mixing in unstable layers. The scheme uses an air parcel plume ascent method to diagnose one of six possible boundary layer ''types,'' each of which has a predetermined K profile (deduced from large-eddy simulations). The scheme determines the magnitudes of the profiles from the turbulent scaling velocities. For stable layers, local Richardson number–based mixing is applied.

A diagnostic scheme (Smith 1990) is used for predicting layer clouds and their water content. It uses a triangular probability density function (PDF) to calculate cloud fraction as a function of gridbox mean saturation. The surface scheme used is a tile scheme [the second Met Office Surface Exchange Scheme (MOSES II)] with nine tile types, a thermal vegetation canopy and four deep soil levels (Cox et al. 1999). Other parametrization schemes include a mass flux convection scheme (Gregory and Rowntree 1990) with convective available potential energy (CAPE)-based closure, a two-stream radiation scheme (Edwards and Slingo 1996), and a mixed-phase precipitation scheme (Wilson and Ballard 1999) with a prognostic ice variable and microphysically based transitions between vapor, liquid, ice, and rain.

b. Case of 14 September 2001 (CUM)

This day was characterized by light northerly flow on the edge of an anticyclone at the site. Initial conditions were clear with cumulus developing during the morning and increasing in fraction during the afternoon before spreading out into a thin layer of 4–5 octa (an octa is one-eighth cloud cover) stratocumulus. During the evening the cloud had the appearance of being decoupled

from the surface, showing the characteristic hexagonal structures of radiatively cooling cloud. During the morning period a layer of stratocumulus/altostratus (at approximately 2-km altitude) advected over the site for a period of about 2 h before moving away to the east. There are, thus, two points to note for comparison with the model: (i) Did it capture the sheet of Sc during the morning? (ii) How well did it simulate the cumulus field?

Figures 1a–1f show tephigrams with observed radiosonde and model forecast profiles (initialized at 0000 UTC). Figure 1a (0700 UTC) shows both the model and observation have the same basic structure, save a few details (i.e., the model surface is too cool, and its humidity between 800 and 650 mb is a smoothed version of the layering seen in the sonde). By 0800 (Fig. 1b), however, the observation shows a moist layer between 900 and 800 mb, capped with a strong, sharp inversion and 4–5-octa stratocumulus. This layer of Sc was present for approximately 2 h and formed the western part of a large cloud sheet covering East Anglia. The model does not represent this layer, showing the same basic structure as at 0700 UTC. Figure 1c shows that by 1200 UTC the inversion was still present, but had descended and warmed, with no cloud present. The inversion is not represented by the model. By 1400 UTC (Fig. 1d) the feature had disappeared, and the observed levels above the boundary layer were again similar to the forecast. Figures 1e–1f show that this remained the case until the end of the period. As a comparison, Fig. 2 shows the model analysis for 1200 UTC, together with the observation. It can be seen that the analysis shows a significantly different profile much closer to the observation than the previous forecast (cf. with Fig. 1c). Importantly, the stratocumulus inversion is represented. It seems plausible that the analysis for the forecast (at 0000 UTC) did not represent the layer and, therefore, the feature, which advected passively, was absent from the forecast.

Figures 1a–1e also depict the development of the boundary layer. Some small cumuli were present before the arrival of the Sc sheet, which halted their development until it started receding at around 1130 UTC. The figures show the model consistently placed the boundary layer inversion base too low. This resulted in predicted temperatures and dewpoints there that were too high and too low, respectively. As a consequence, the model predicted no convective cloud at all, significantly in error to the observations. The observed and model boundary layer cloud evolution is shown in Fig. 3.

Model profiles were also examined at the remote sonde location, approximately 60 km upwind of Cardington. These data showed a very similar comparison to that at the main site, including no representation of the Sc layer at 800 mb. It was noted the model did produce layer cloud farther eastward, and so a profile was examined there. However, this cloud was seen to originate in the boundary layer at approximately 970 mb. No cloud or inversion feature was seen near 800 mb.

In summary, the model failure to depict the layer of Sc is likely due to errors in the analysis, which is consistent with the following discussion in section 4. The failure to depict the cumulus layer may be due to the limited vertical resolution, and this will be considered in more detail later (see section 5). However, errors due to limited gridpoint resolution do not account for all of the error because the analysis shown in Fig. 2 does show a better representation of the boundary layer than the forecast. Some of the errors seen in this figure (e.g., at 875 mb) also indicate other sources of error than gridpoint resolution.

c. Case of 25 September 2001 (SCC)

As described previously, this day was characterized by a morning fog layer that lifted into stratus/stratocumulus and subsequently broke into clear-sky conditions, with the occasional cumulus. Figures 4a–4d show model and observed tephigrams for the period when cloud was thinning. At 0700 UTC fog was present. By 1200 UTC 8 octa of thin Sc was present. Figures 4a–4b show reasonable agreement between the model and observations in the boundary layer, but the inversion is not modeled as well. The inversion is also poorly resolved in Figs. 4c–4d. We note that the limited stability there (in conjunction with boundary layer heating) would allow the model to develop an unnaturally deep boundary layer that could lead to inaccurate cloud forecasts. However, that did not occur in this case due to the limited boundary layer heating seen in the model. Figures 4c–4d show sonde data depicting significant warming occurring, causing cloud to thin and increase significantly in height. In contrast, the model shows very limited development with only a slight warming and the cloud remaining thick. The cloud liquid water evolution measured by a microwave radiometer is compared to the model in Fig. 5. This shows that model values were higher than those observed, indicating that forecast cloud was too thick, which could explain the slower rate of heating predicted. Figure 6 shows the 1200 UTC analysis compared to observations. In contrast to the forecast shown in Fig. 4d, the analysis has produced an upper boundary layer that is too warm and dry (relative humidity), which would lead to an underestimate of cloud. Note also that the inversion base is too low, again consistent with limited vertical resolution (see section 5).

In summary the boundary layer conditions were better forecast initially for this case, and the cloud top was reasonably well placed. However the inversion was poorly resolved. The forecast errors increased during the period, and this appears to be due mainly to the forecast not heating the boundary layer enough, rather than being caused by poor resolution. As with CUM, the analysis at 1200 UTC showed a significantly dif-

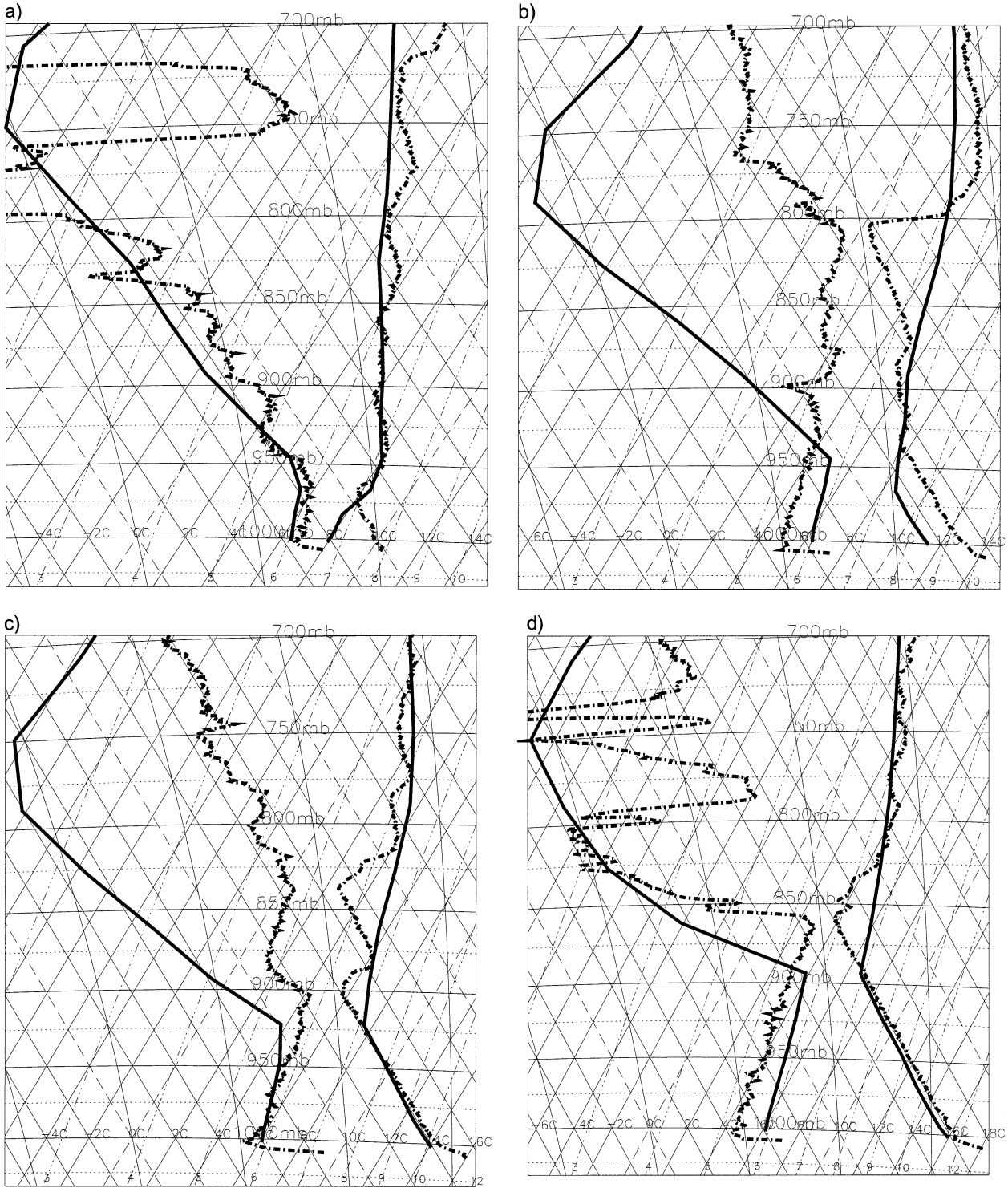

FIG. 1. Tephigrams showing comparison of observed (broken line) and forecast profiles for CUM at (a) 0700, (b) 1000, (c) 1200, (d) 1400, (e) 1600, (f) 1800 UTC. Pressure lines are approximately horizontal in these diagrams. Temperature increases downward to the right and potential temperature upward to the right; intervals are every 2°C. The curved lines are saturated adiabats and are usually followed closely by saturated boundary layer air. Dashed lines are lines of saturated specific humidity; air above and to the left is saturated at that value. Model values are plotted as solid lines and observations dashed. In each case the temperature profile lies to the right and dewpoint to the left. Where these two lines meet indicates cloud, and when farther apart, indicates lower relative humidity.

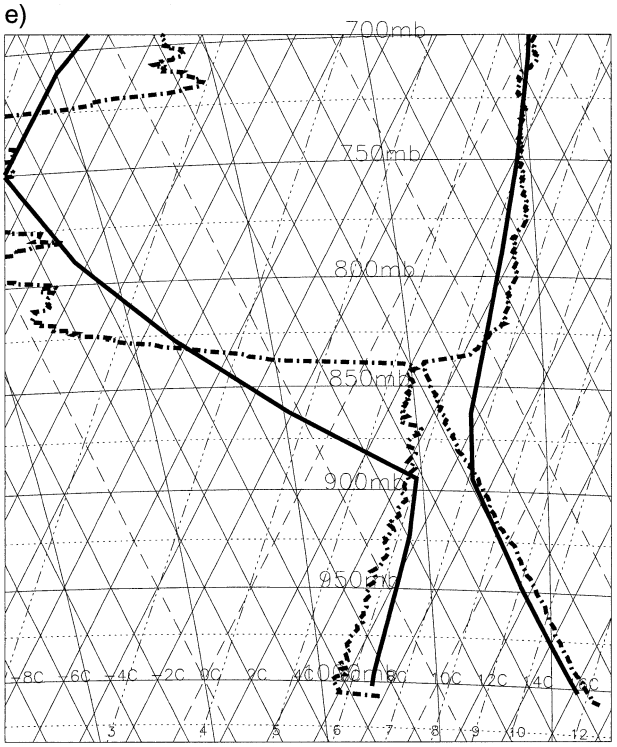

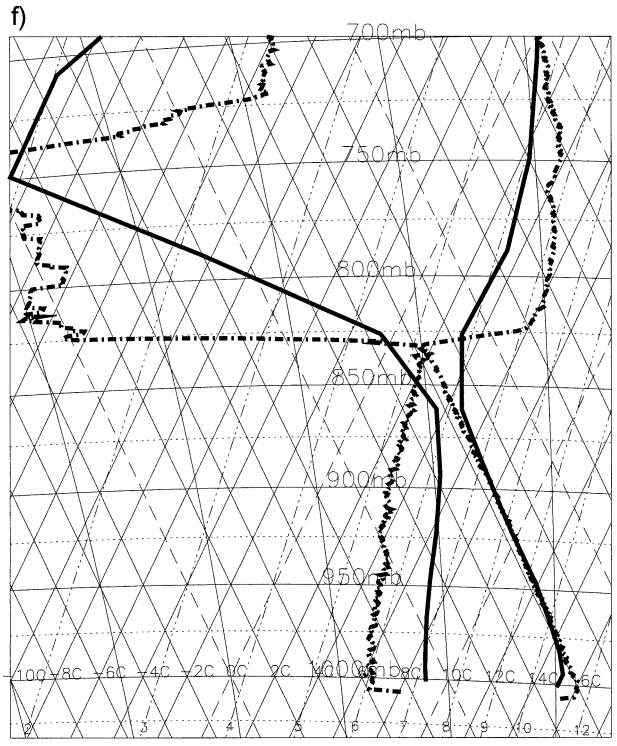

FIG. 1. (*Continued*)

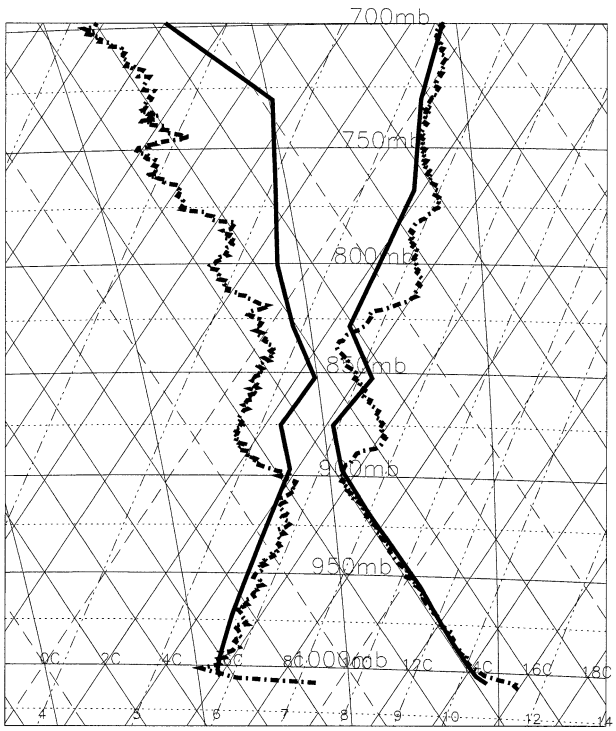

FIG. 2. Tephigram (as Fig. 1) showing observed (broken line) and model analysis profiles for 1200 UTC for CUM.

ferent profile to the earlier forecast, and also some evidence of low resolution.

d. Case of 2 November 2001 (SCQ)

This day was characterized by a large anticyclone over the United Kingdom with westerly to northwesterly flow at the site. Satellite images for the period (not presented) showed that a large area of stratocumulus cloud was present over the middle of the United King-

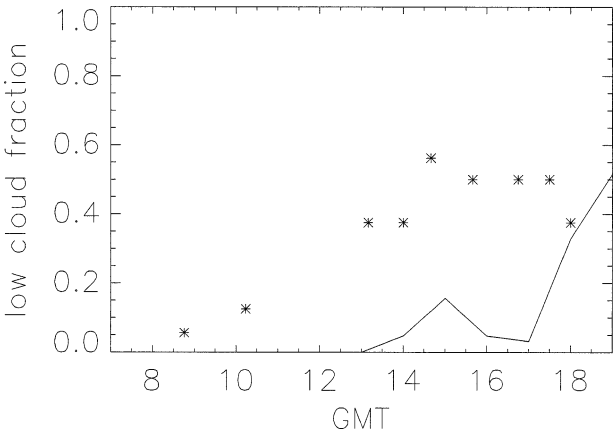

FIG. 3. Observed (asterisks) and modeled boundary layer cloud fraction throughout the period for CUM. Model values are for layer cloud. No convective cloud was forecast.

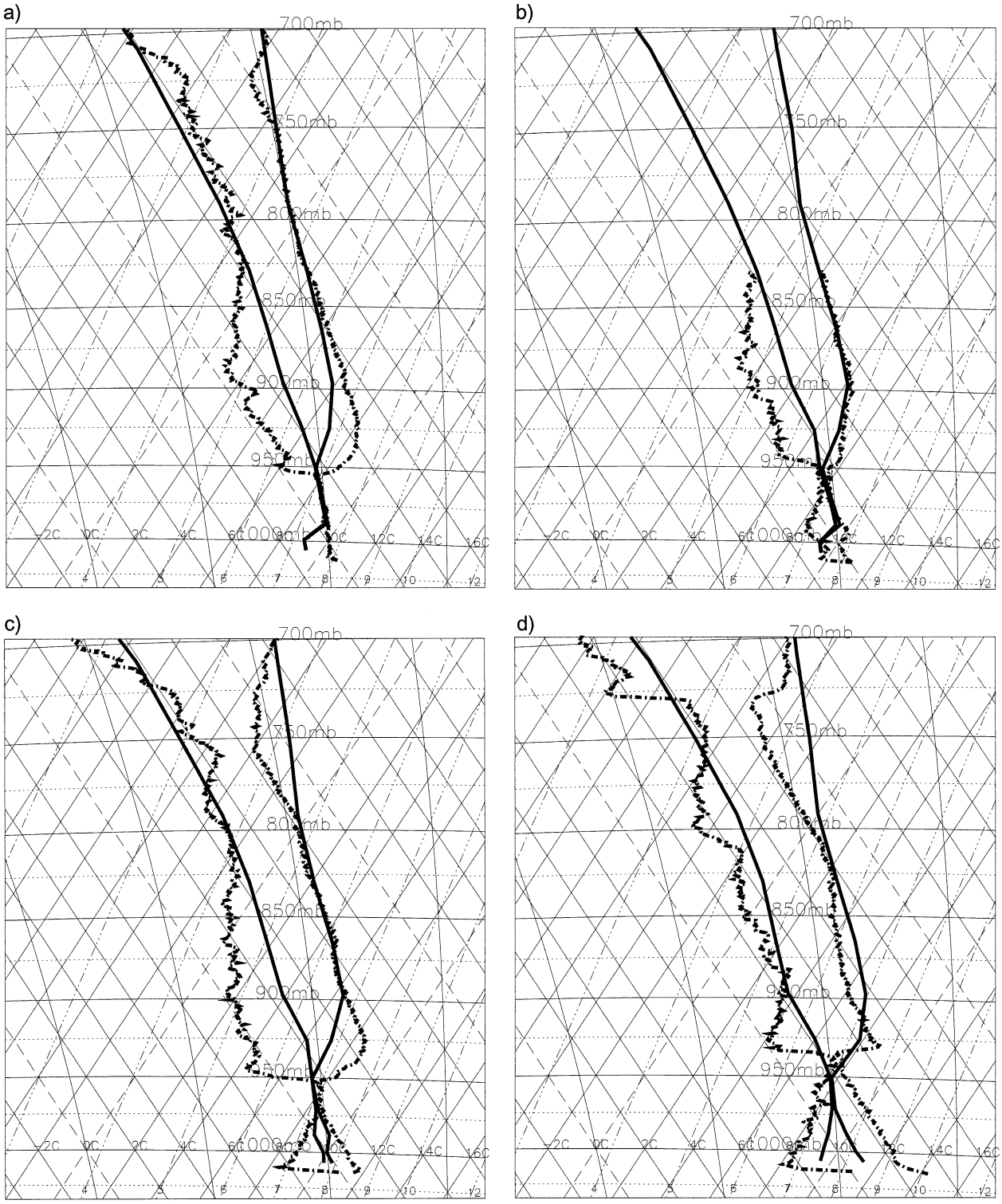

FIG. 4. Tephigrams (as in Fig. 1) showing comparison of observed (broken line) and forecast profiles for SCC at (a) 0700, (b) 0800, (c) 1000, (d) 1200 UTC.

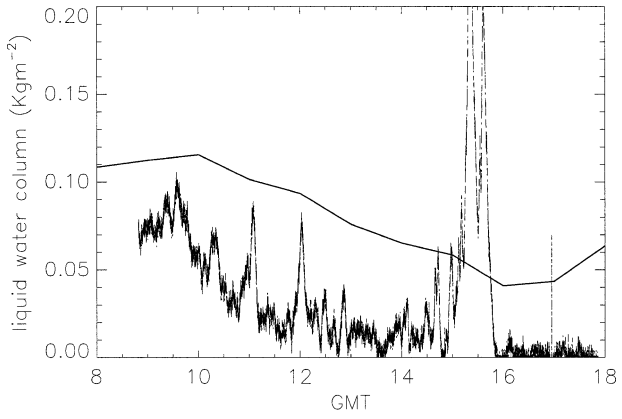

FIG. 5. Observed (broken line) and modeled liquid water path for SCC. The error in the observations is approximately 0.01 kg m^{-2}.

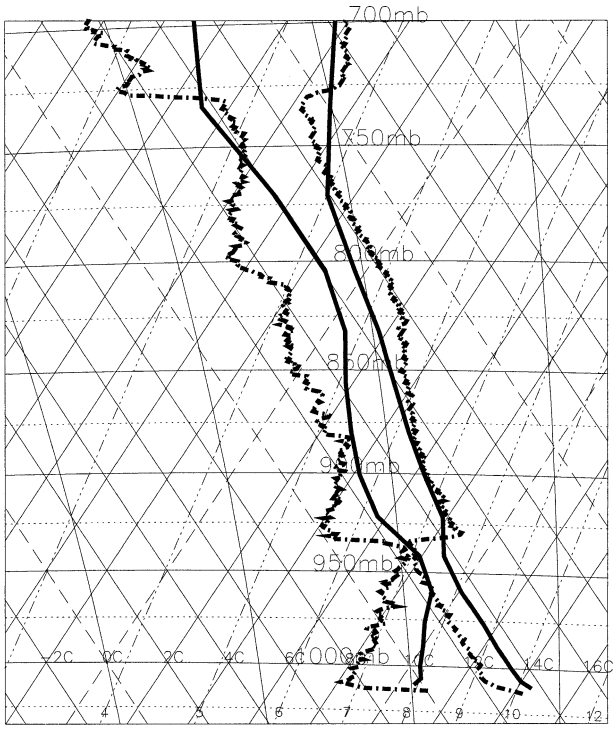

FIG. 6. Tephigram (as in Fig. 1) showing observed (broken line) and model analysis profiles for 1200 UTC for SCC.

dom, stretching from Wales in the west over to East Anglia and out over the North Sea. To the south over southern England there was clear air. The cloud appeared to be largely decoupled from the surface, apart from a brief period during early afternoon when a few small cumulus (Cu) were seen to develop and penetrate into it. In fact the cloud-cover evolution at the site was governed by advection, which was limited to cloud thinning early in the period when the clear region in the south approached the site, placing it near the edge of the stratocumulus sheet. The cloud subsequently thickened as this edge receded and, thereafter, little change was observed in the cloud structure. The cloud was relatively thin (1–200 m) capped by a strong, shallow dry inversion.

Figures 7a–7d show examples of forecast and observed tephigrams for the period. The most striking feature of these is the rather poor model representation of the inversion base and cloud region, which appears to be absent. Temperatures in the region are too warm and relative humidity is too low. As a consequence, the model produces very little cloud during the period. Figure 8 shows the observed and predicted liquid water path. The observations show decreasing values during the morning as the cloud edge advected toward the site, with increasing values thereafter as it receded (the period between approximately 1040 and 1140 UTC is erroneous due to an instrument temperature controller error). The model fails to produce any liquid water until the end of the period, and this is significantly underestimated (see bottom right in the figure). Figure 9 shows the model 1200 UTC analysis tephigram compared to the observation. This gives a much better fit, but we note that there is still significant error in location of the inversion base. As seen previously, it is too low, warm, and dry (relative humidity). As discussed for CUM, the errors seen here are not solely due to gridpoint resolution. Examination of the figures reveals that the quantities at model levels in the region of the inversion base could be placed more accurately, and, therefore, the major errors in this case do not appear to be governed by gridpoint resolution. Figure 9 indicates that at least some of this error originates in the assimilation cycle in a similar manner to Fig. 2.

Model profiles were also compared at the remote sonde location approximately 60 km upwind. These comparisons gave very similar results to those at the main site.

In summary, all three cases show evidence of low resolution and/or errors in data assimilation. Cases SCQ and CUM appear to be particularly affected. It is noted that during assimilation of a radiosonde profile it is interpolated using vertically aligned error covariance matrices that are based on a standard profile (Schlatter 2000). This means that when an observed profile shows a feature (such as an inversion) that is not represented in the standard profile, the interpolation acts to smooth out and spread the feature in the vertical. This process could explain the poorly resolved inversions seen in this comparison.

4. Estimation of radiosonde random errors

When comparing radiosonde and model wind profiles one needs to assess the errors of the former before conclusions about model accuracy can be made. In particular, model profiles represent an average over a finite area—typically 50–400 km^2 for mesoscale models, and a radiosonde measures at a localized point. This means that comparisons between the two will be invalid if the

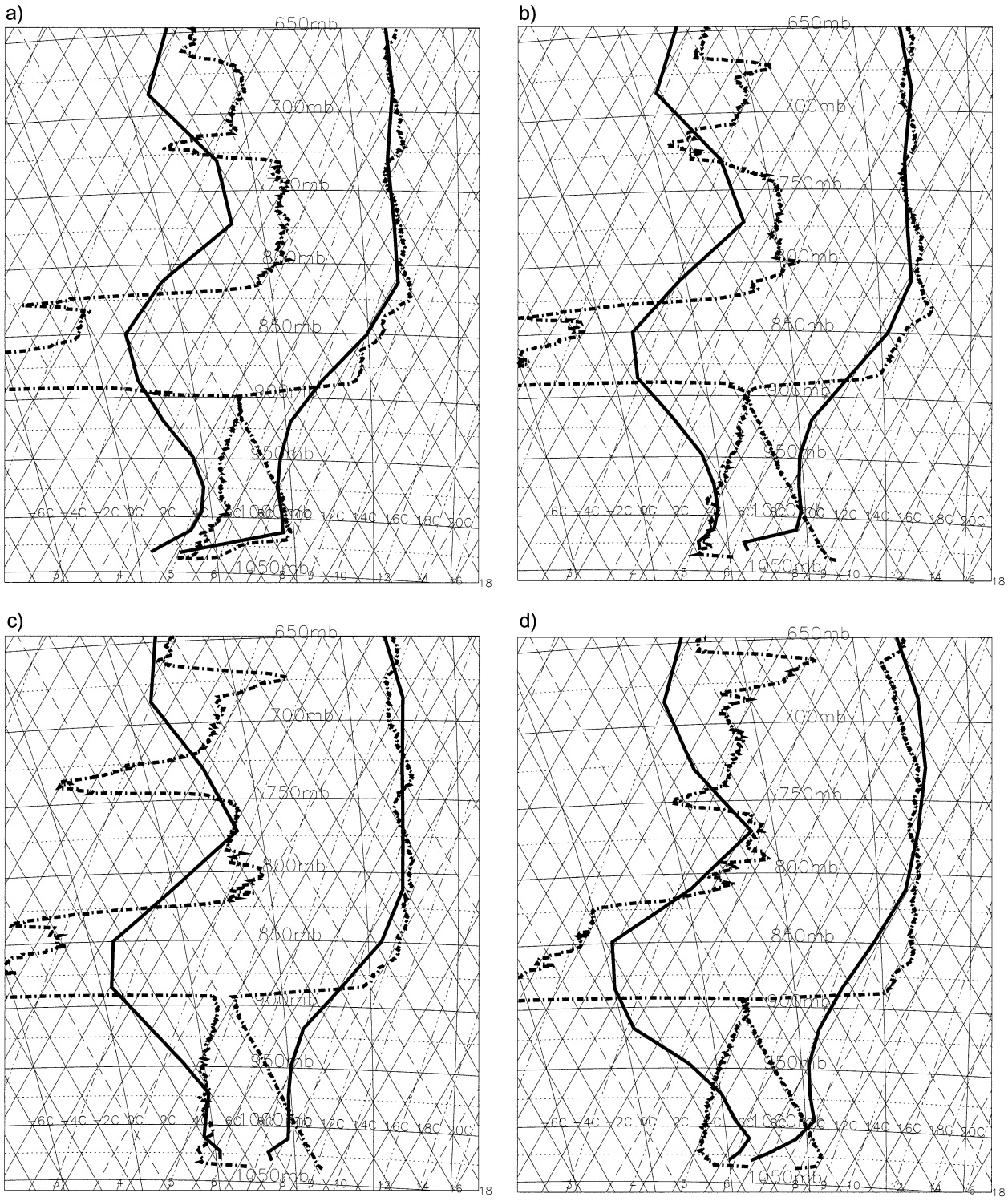

FIG. 7. Tephigrams (as in Fig. 1) showing comparison of observed (broken line) and forecast profiles for SCQ at (a) 0700, (b) 1100, (c) 1400, (d) 1800 UTC.

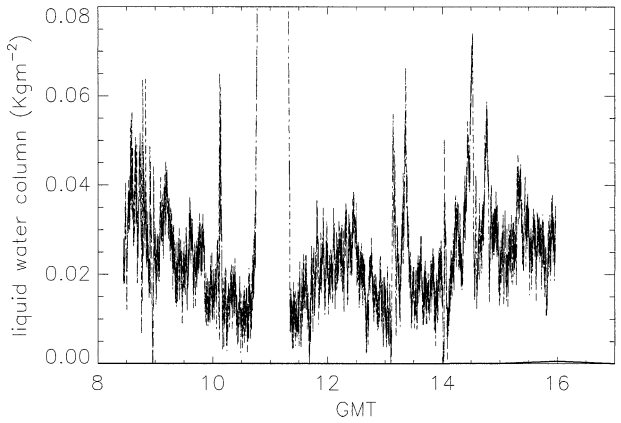

FIG. 8. Observed (broken line) and modeled (extreme bottom right) liquid water path for SCQ.

localized point has significantly different properties to the grid-box mean. In this section characteristic radiosonde boundary layer random errors on scales up to 20 km are deduced for three generic boundary layer types using tethered balloon data. The three generic boundary layers match the case study types as follows (presented in section 3):

1) Quiescent layers of stratus and stratocumulus: characterized by low levels of turbulence, and often decoupled from the surface (case SCQ);
2) Convective stratocumulus: characterized by moderate levels of turbulence and normally coupled to the surface (case SCC);
3) Cumulus fields: normally characterized by high levels of turbulence (case CUM).

Tethered balloon data consist of time series of temperature and humidity from turbulence probes (logged at 4 Hz) placed in the boundary layer near the inversion base (see Price and Wood 2002, for examples of measured variances and comparison with aircraft data). Because a radiosonde may effectively intercept these time series at any point, then its random error can be equated to the standard deviation of the time series, if it is assumed that the time series is in equilibrium. Data are typically collected over periods from one-half to 1 h, so that for some convective cases in situ development will occur and the time series will not solely represent spatial variations (the standard deviation measured will be artificially widened). However, in convective cases the standard deviations are normally large (due to in situ turbulence), and so the increase is relatively small. The time series are, thus, dominated by spatial variations only and can be used to estimate the sonde random error to reasonable accuracy. Results are presented in Table 1; average measured standard deviations in temperature and total specific humidity q_t together with the length scale of the observations. The length scale is defined as the mean wind speed multiplied by the duration of the time series.

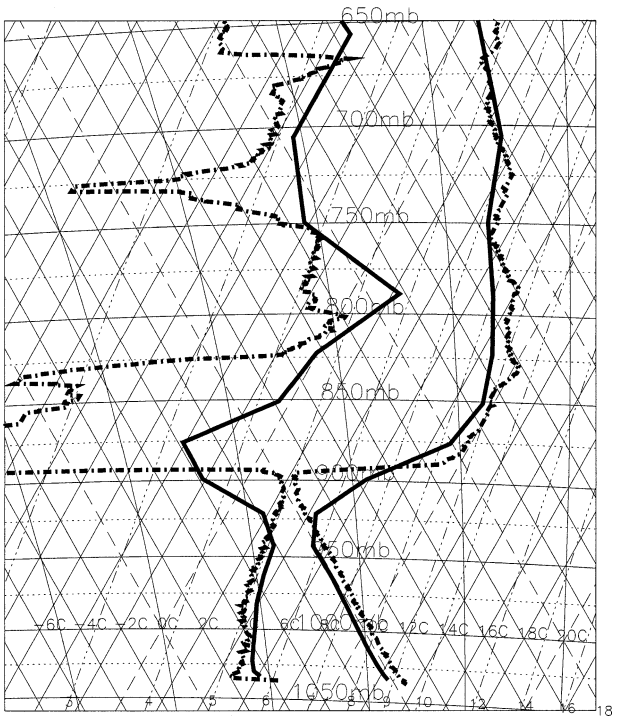

FIG. 9. Tephigram (as in Fig. 1) showing observed (broken line) and model analysis profiles for 1200 UTC for SCQ.

The values for standard deviation shown in Table 1 reveal a trend where the values are proportional to the level of turbulence, consistent with the findings of Price (2002), who also showed that they were only weakly proportional to the length scale of the observation (for scales up to 20 km). The values for the quiescent cloud layers are smallest, and those for the cumulus fields are largest. These random errors can be equated to cloud fraction errors using a simple cloud parametrization. The scheme used assumes a triangular PDF for saturation deficit $q_t - q_{\text{sat}}$ (denoted S; q_t is the total specific humidity and q_{sat} is the saturated specific humidity). This quantity effectively defines the thermodynamic distance a grid box is from the mean saturation point ($S = 0$), and is used in several cloud parametrizations (Gregory et al. 2002). The width of the PDF has a standard deviation of 0.30 g kg^{-1}, which is the average value found by Price and Wood (2002) when they examined a large amount of tethered balloon and aircraft data taken in the boundary layer. It is found that the associated cloud fraction errors for stratocumulus are unlikely to be greater than 1 octa. For cumulus they are likely to be greater than this. In particular, the random error in humidity is significant. A final point evident in Table 1 is that the ratio of the standard deviation of humidity to temperature appears to increase from approximately 1:3 to 1:1 as convective activity increases. In convective cases one can expect more direct transport of less diluted surface air into the upper boundary layer in thermal plumes, creating relatively larger variance there. The fact that

TABLE 1. Tethered balloon data showing average values of std dev in absolute total humidity σ_{qt} and temperature σ_T measured near the inversion base for the three types of boundary layer defined in the text. Each day contains, on average, two measurements of standard deviation. Figures in parentheses are the difference between observed and forecast temperature and specific humidity for the corresponding case studies described in the text.

Boundary layer	No. of days	Length scale (km)	σ_{qt} (g kg^{-1})	σ_T (°C)
Quiescent Sc	4	8.9	0.05 (0.3)	0.16 (6.0)
Convective Sc	4	16.9	0.17 (0.3)	0.40 (0.4)
Cumulus	5	14.9	0.65 (1.0)	0.60 (2.5)

humidity variance increases more rapidly suggests that humidity transport there becomes more efficient for convective cases, or that the temperature variance created is quickly being reduced by buoyancy forces (as one would expect).

We also note here that the instrumental errors for the type of sonde (Vaisala RS80-15GH) used in this study are similar to or smaller than the figures for random error, so that the random error can be expected to dominate in most cases. The temperature error is quoted as 0.2°C, and humidity probable error is 0.2 g kg^{-1}, unless the measurement is taken in cloud, when saturation can be assumed and the error becomes dependent on temperature only, and reduces to 0.05 g kg^{-1}.

Table 1 also contains figures (in brackets) for the difference between model forecast and sonde temperature and humidity at the boundary layer inversion base for the three case studies presented in section 3. Comparing these figures with the corresponding sonde random errors we see that the observed differences are mostly significantly larger than the random errors. We conclude, therefore, that the model forecast errors are significant.

5. Vertical resolution

As discussed in section 3, results of the comparison show that the model did not represent the fine vertical structure seen in the observations. As stated, this may be due to both errors in the data assimilation for the analysis field and the relatively poor vertical grid resolution of the model. Previous studies have demonstrated the importance of increased vertical resolution on forecasting various quantities, including cloud (e.g., Bushell and Martin 1999; Menon et al. 2003). While it is logical that poorer vertical resolution is likely to degrade the accuracy of forecast cloud parameters, it is not obvious how important this will be, or what optimum resolution is required in order to provide an accurate forecast. In this section a simple method is used to deduce the accuracy of predicted cloud fraction as a function of vertical resolution. We consider higher resolutions than previous studies down to 30 m.

Sonde data typically have good vertical resolution in the range of 5–15 m (depending on ascent rate). By degrading the resolution of a profile using a box-car-averaging method, it is possible to compare temperature and humidity at the inversion base and quantify their variation with changing resolution. Thermodynamic quantities used in cloud parametrization can also be computed and compared, in particular, the mean grid-box saturation deficit *S*.

TABLE 2. Showing average absolute errors for inversion base parameters for 18 profiles at four vertical resolutions; *T* is temperature (°C), *P* is pressure (mb), q_t and q_{sat} are total and saturation specific humidity (g kg^{-1}), *S* is saturation deficit (g kg^{-1}), and *C* is cloud fraction (not in octas).

Resolution (m)	*T*	*P*	q_t	q_{sat}	*S*	*C*
30	0.06	1.3	0.08	0.02	0.09	0.06
60	0.18	2.7	0.08	0.06	0.09	0.07
120	0.48	6.3	0.08	0.14	0.18	0.15
240	1.14	14.5	0.25	0.38	0.53	0.25

Four resolutions were examined: 30, 60, 120, and 240 m. Six sample sondes were used from each of the three case studies. Average absolute errors for all of the data for various quantities at the four resolutions are shown in Table 2. This table also contains errors for predicted cloud fraction made using the simple parametrization described in section 4. The results in Table 2 show that resolution does have a significant impact on predicted cloud fraction, and indicates that to reduce errors to less then 1 octa (i.e., 0.125), resolutions higher than 120 m are required. The results also suggest that resolutions better than 60 m are not necessary, because the difference between 30 and 60 m is small. Note that errors for 240-m resolution, which is a value typical for current mesoscale models, are quite large. In nearly all of the cases, reducing the resolution lowered the inversion base and increased the saturation deficit *S*, thereby reducing predicted cloud fraction. Most predicted cloud fractions at a low resolution were, therefore, underestimated. The reduced profiles appeared similar in structure to the model profiles presented in section 3. A typical example of profile appearance at different degraded resolutions (original profile, 60 and 240 m) is shown in Fig. 10.

6. Summary

A series of three observational case study experiments have been used to assess the performance of the Met Office mesoscale model in representing boundary layer profiles, with particular attention to its prediction of cloud. It was found that the modeled vertical profiles deviated enough from the observed ones to cause significant errors in predicted cloud fraction. In particular, the inversion base and/or boundary layer top was often placed too low and, consequently, was too warm with too large a dewpoint depression. This resulted in a general underestimation of cloud cover. The results indicate

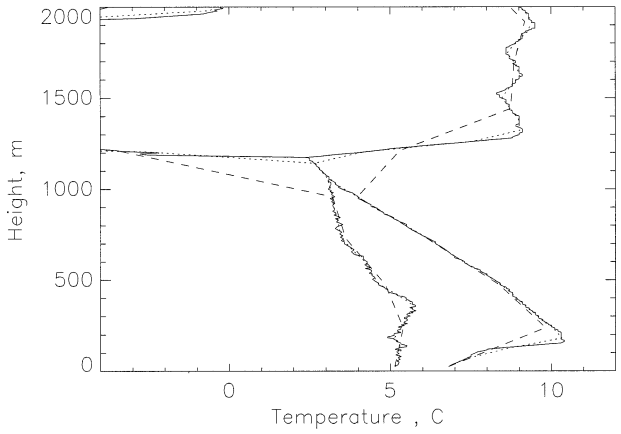

FIG. 10. Example plot showing comparison between a vertical profile averaged over different vertical intervals: original profile (solid line), 60 m (dotted line), 240 m (dashed line). As with the tephigram plots, both temperature and dewpoint are plotted for each profile.

that limited vertical resolution and errors in data assimilation (i.e., the analysis fields) were the major cause of error in two of the cases. The other case also showed evidence of these effects, but the main forecast errors there originated during the forecast. This indicates that for the cases considered here, the most likely cause of error in the forecast cloud fraction originates in the data assimilation process or is inherent in the limited vertical resolution of the model. When this occurs, in practice, cloud parameterizations are likely to achieve only a limited accuracy.

A simple study has estimated the required vertical resolution in order to resolve the thermal structure with enough precision to accurately forecast cloud fraction. The results suggest that 30–60-m resolution is required to reduce predicted cloud fraction error to less than 1 octa. It is noted that this figure is significantly higher than in the current generation of mesoscale models, which have typically 200 m or poorer resolution in the boundary layer.

In conclusion, the accuracy of predicted cloud variables is likely to increase as data assimilation methods improve and higher vertical resolution models become more prevailent.

Acknowledgments. We would like to thank the staff at the Met Research Unit, Cardington, for their assistance in collecting the observational data used in this study. The helpful comments of three reviewers are also appreciated.

REFERENCES

Bushell, A. C., and G. M. Martin, 1999: The impact of vertical resolution upon GCM simulations of marine stratocumulus. *Climate Dyn.,* **15,** 293–318.

Cox, P. M., R. A. Betts, C. Bunton, R. L. H. Essery, P. R. Rowntree, and J. Smith, 1999: The impact of new land surface physics on the GCM simulation of climate and climate sensitivity. *Climate Dyn.,* **15,** 183–203.

Edwards, J. M., and A. Slingo, 1996: Studies with a flexible new radiation code. Part 1. Choosing a configuration for a large-scale model. *Quart. J. Roy. Meteor. Soc.,* **122,** 689–719.

Gregory, D., and P. R. Rowntree, 1990: A mass flux convection scheme with representation of cloud ensemble characteristics and stability-dependent closure. *Mon. Wea. Rev.,* **118,** 1483–1506.

——, D. Wilson, and A. Bushell, 2002: Insights into cloud parametrization provided by a prognostic approach. *Quart. J. Roy. Meteor. Soc.,* **128,** 1485–1504.

Lock, A. P., A. R. Brown, M. R. Bush, G. M. Martin, and R. N. B. Smith, 2000: A new boundary layer mixing scheme. Part 1: Scheme description and single-column model tests. *Mon. Wea. Rev.,* **128,** 3187–3199.

Menon, S., and Coauthors, 2003: Evaluating aerosol/cloud/radiation process parameterizations with single-column models and Second Aerosol Characterization Experiment (ACE-2) cloudy column observations. *J. Geophys. Res.,* **108,** 4762, doi:10.1029/2003JD003902.

Price, J. D., 1999: Observations of stratocumulus cloud break-up over land. *Quart. J. Roy. Meteor. Soc.,* **125,** 441–468.

——, 2002: A semi-empirical parametrization for total in situ specific humidity standard deviation derived from tethered balloon observations. *Quart. J. Roy. Meteor. Soc.,* **128,** 733–739.

——, and R. Wood, 2002: Comparison of probability density functions for total specific humidity and saturation deficit humidity, and consequences for cloud parametrization. *Quart. J. Roy. Meteor. Soc.,* **128,** 2059–2072.

Ricard, J. L., and J. F. Royer, 1993: A statistical cloud scheme for use in an AGCM. *Ann. Geophys.,* **11,** 1095–1115.

Schlatter, T. W., 2000: Variational assimilation of meteorological observations in the lower atmosphere: A tutorial on how it works. *J. Atmos. Sol. Terr. Phys.,* **62,** 1057–1070.

Smith, R. N. B., 1990: A scheme for predicting layer clouds and their water content in a general circulation model. *Quart. J. Roy. Meteor. Soc.,* **116,** 435–460.

Sommeria, G., and J. W. Deardorff, 1977: Subgrid-scale condensation in models of nonprecipitating cloud. *J. Atmos. Sci.,* **34,** 344–355.

Staniforth, A., A. White, N. Wood, J. Thuburn, M. Zerroukat, E. Cordero, and T. Davies, 2002: The joy of UM5.2—Model formulation. Met Office Unified Model Doc. Paper 15, 250 pp.

Tiedtke, M., 1993: Representation of clouds in large-scale models. *Mon. Wea. Rev.,* **121,** 3040–3061.

Wilson, D. R., and S. P. Ballard, 1999: A microphysically based precipitation scheme for the U.K. Meteorological Office Unified Model. *Quart. J. Roy. Meteor. Soc.,* **125,** 1607–1636.